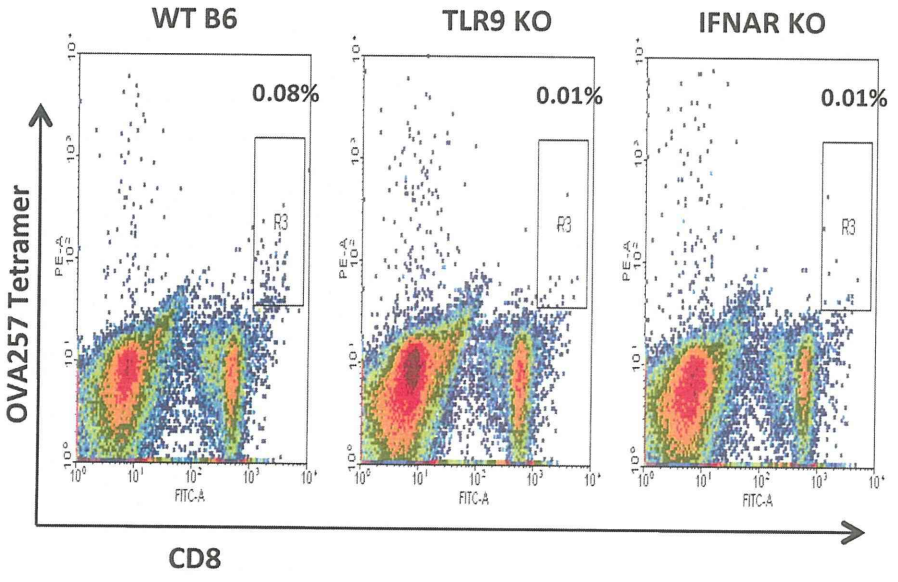

図1. TLR9およびIFNAR依存的CD8T細胞誘導

厚生労働科学研究費補助金（医療機器開発推進研究事業）
分担研究報告書

CTL誘導型エボラ出血熱ワクチンの臨床応用に向けた検討

分担研究者　松井政則　埼玉医科大学微生物学教室　准教授

研究要旨

ペプチド結合リポソームを用いた CTL 誘導型エボラ出血熱ワクチンの開発に向けて、昨年度までにワクチン抗原となりうる HLA-A2 および HLA-A24 拘束性のエボラウイルス由来 CTL エピトープを同定した。本年度は、昨年度同定した HLA-A24 拘束性 CTL エピトープのペプチドを合成しリポソームに結合させてペプチド結合リポソームを作製し、HLA-A24 トランスジェニックマウスにおける CTL 誘導能を検討した。また、HLA-A2 および HLA-A24 拘束性のエボラウイルス由来 CTL エピトープが、エボラウイルス構造タンパク質 L の部位に多く存在したことから、L および HLA-A2 または HLA-A24 を発現する細胞株を樹立し、この細胞株が提示する内在性抗原をペプチド結合リポソーム免疫によって誘導された CTL が認識するか否かを検討した。その結果、誘導された CTL が内在性抗原を認識するような CTL エピトープが複数存在することが明らかとなった。

A．研究目的

本研究は、現在、効果的な予防・治療法がないエボラ出血熱に対する CTL 誘導型ワクチンの開発を目的としている。昨年度までの検討で、エボラウイルスに対する HLA-A2 の CTL エピトープを同定し、そのエピトープを結合させたペプチド結合リポソームが、ペプチド特異的 IFN-$g^{+}CD8^{+}$T 細胞および CTL を効率よく誘導できることが明らかとなった。本年度は、昨年度同定した HLA-A24 の CTL エピトープを結合させたペプチド結合リポソームの CTL 誘導能を検討した。さらに、構造タンパク質 L および HLA-A2 または HLA-A24 を発現する細胞株を用いて、ペプチド結合リポソームによって誘導された CTL が内在性抗原を認識するか否かを検討した。

B．研究方法

1）*in vivo* killing 活性の測定：HLA-A24 拘束性 CTL エピトープ結合リポソームによる CTL 誘導能を、*in vivo* CTL アッセイによって検討した。

2）^{51}Cr 遊離試験：CTL エピトープ結合リポソームを HLA-A2 または HLA-A24 トランスジェニックマウスに免疫した後に脾細胞を回収し、それぞれのペプチドで刺激したものをエフェクター細胞とした。トランスフェクタントは ^{51}Cr で標識し、標的細胞とした。エフェクター細胞と標的細胞を比率を変えて混和し、遊離した ^{51}Cr を測定した。

（倫理面への配慮）

マウスは、埼玉医大・実験動物管理運営規定に基づき飼育され、日本動物学会が定めた、苦痛の軽減、安楽死等に配慮した指針に従って実験を行った。

C．研究結果

1）HLA-A24 拘束性 CTL エピトープによって誘導される CTL 活性の測定：昨年度同定された 9 種類のエボラウイルス由来ペプチドを結合させたペプチド結合リポソームすべてにおいて、killing 活性の誘導が認められた（図 1）。

2）エボラウイルス構造タンパク質 L および HLA-A2 または HLA-A24 を発現する細胞株を樹立した（図 2）。

3）^{51}Cr 遊離試験：HLA-A2 拘束性 CTL エピトープ 6 種類のうち 2 種類（L-209, L-932）、HLA-A24 拘束性 CTL エピトープ 9 種類のうち 7 種類（L-1087, L-1359, L-1847, L-1939, L-1943, L-2000, L-2046）のペプチド結合リポソームによって誘導された CTL が、内在性抗原を認識することが明らかとなった（図 3 及び図 4）。

D．考察

昨年度同定された HLA-A24 拘束性のエボラウイルス由来 CTL エピトープを結合したリポソームによって誘導された CTL は、ペプチド特異的な killing 活性を有することが示された。また HLA-A2 拘束性 CTL エピトープ 6 種類

のうち 2 種類、HLA-A24 拘束性 CTL エピトープ 9 種類のうち 7 種類のペプチド結合リポソームによって誘導された CTL が内在性抗原を認識することが明らかとなった。

E．結論

エボラワクチンのワクチン抗原となりうる HLA-A2 および HLA-A24 拘束性のエボラウイルス由来 CTL エピトープが同定され、エピトープ結合リポソームによる IFN-$g^{+}CD8^{+}$T 細胞、CTL 誘導能が明らかとなった。また内在性抗原を認識する CTL を誘導するエピトープが複数明らかとなり、エボラワクチン候補物質となりうる可能性が示唆された。

F．研究発表

1．論文発表

該当無し

2. 学会発表

該当無し

G．知的財産権の出願・登録状況（予定を含む。）

1．特許出願

該当無し

2．実用新案登録

該当無し

3．その他

該当無し

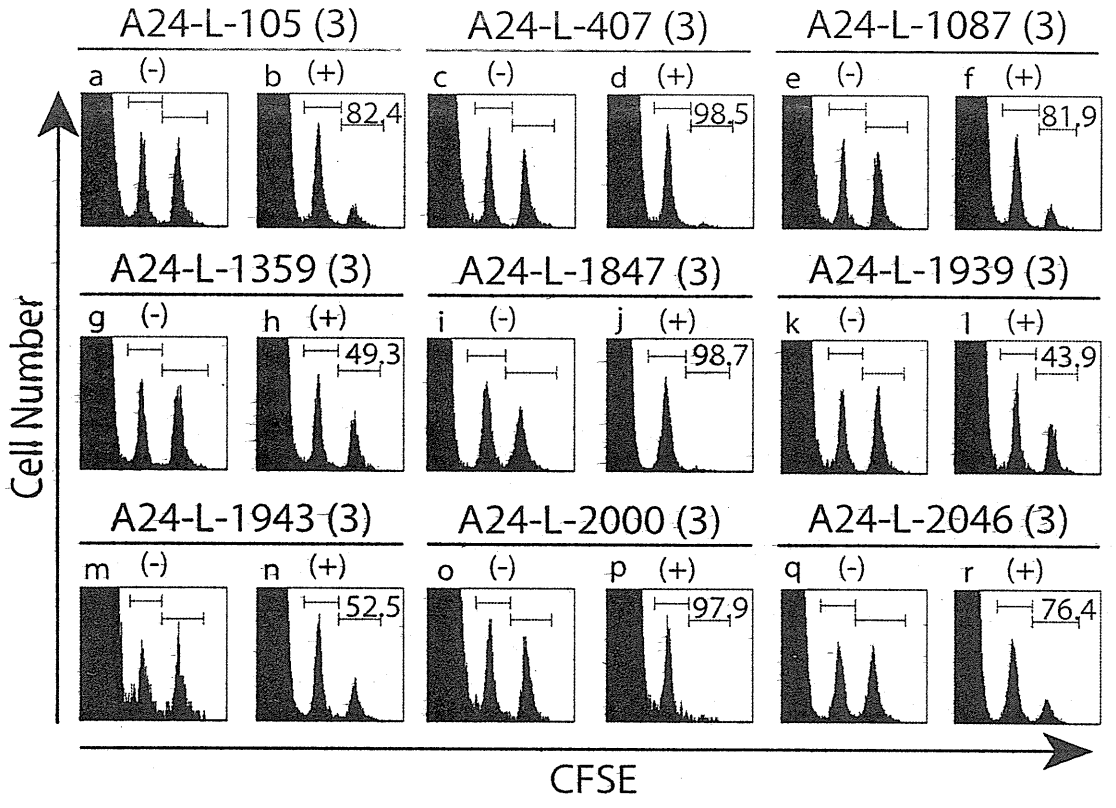

図１　HLA-A24拘束性ペプチド結合リポソームによるCTL誘導
9種類のペプチド結合リポソームをHLA-A24マウスに免疫し、1週間後に、in vivo CTL assayを行い、
ペプチド特異的なkilling活性を測定した。(-)は非免疫群、(+)は免疫群、カッコ内の数値は免疫回数を示す。
ヒストグラム内の数値は% Specific Lysisを示す。

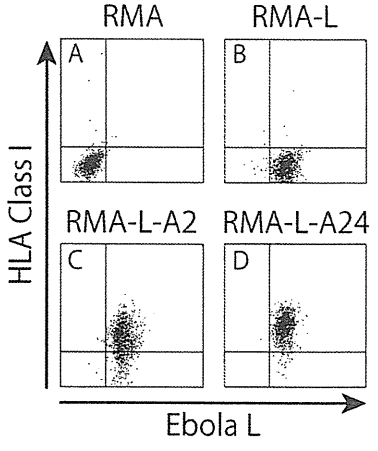

図２　HLA-A2またはA-24およびエボラウイルスLタンパク質発現トランスフェクタントの樹立
RMA細胞にLタンパク質およびHLA-A2またはA24をトランスフェクションし、その発現を
フローサイトメトリーで確認した。

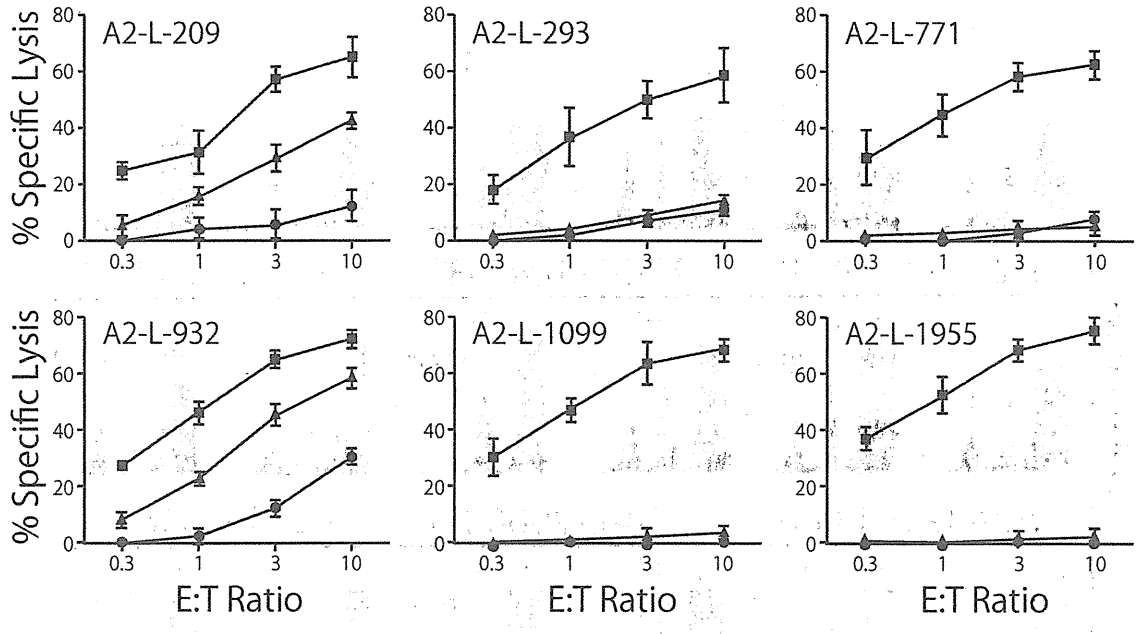

図３　HLA-A2拘束性CTLエピトープ結合リポソーム免疫マウスにおける内在性Lタンパク質の認識
▲はRMA-L-A2細胞、■はペプチドをパルスしたRMA-A2細胞、●はペプチドをパルスしていないRMA-A2細胞を標的細胞とした。

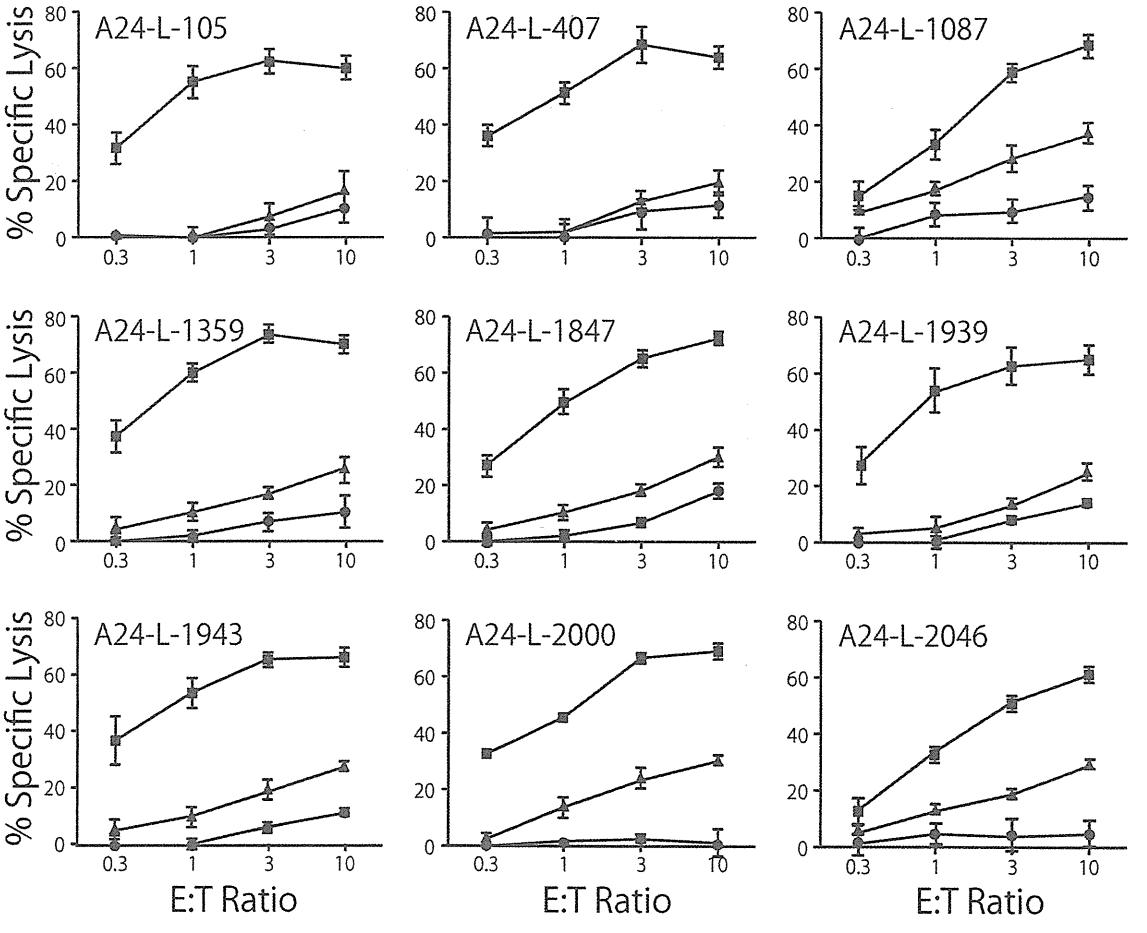

図４　HLA-A24拘束性CTLエピトープ結合リポソーム免疫マウスにおける内在性Lタンパク質の認識
▲はRMA-L-A24細胞、■はペプチドをパルスしたRMA-A24細胞、●はペプチドをパルスしていないRMA-A2細胞を標的細胞とした。

Ⅲ.　研究成果の刊行に関する一覧表

書籍

該当なし

雑誌

発表者氏名	論文タイトル名	発表誌名	巻号	ページ	出版年
Numajiri-Haruki A, Naito T, Nishie T, Saito S, Nagata K.	Interferon-inducible antiviral protein MxA enhances cell death triggered by endoplasmic reticulum stress.	J. Interferon Cytokine Res.	31	847-856	2011
Wakai C, Iwama M, Mizumoto K, Nagata K.	Recognition of cap structure by influenza B virus RNA polymerase is less dependent on the methyl residue than recognition by influenza A virus polymerase.	J. Virol.	85	7504-7512	2011
Kawaguchi A, Momose F, Nagata K.	Replication-coupled and host factor-mediated encapsidation of the influenza virus genome by viral nucleoprotein.	J. Virol.	85	6197-6204	2011
Mori K, Haruyama T, Nagata K.	Tamiflu-Resistant but HA-Mediated Cell-to -Cell Transmission through Apical Membranes of Cell-Associated Influenza Viruses.	PLoS ONE	6	e28178	2011
Simulundu, E., Ishii, A., Igarashi, M., Mweene, A.S., Suzuki, Y., Hang'ombe, B.M., Namangala, B., Moonga, L., Manzoor, R., Ito, K., Nakamura, I., Sawa, H., Sugimoto, C., Kida, H., Simukonda, C., Chansa, W., Chulu, J., and Takada, A.	Characterization of influenza A viruses isolated from wild waterfowls in Zambia.	J. Gen. Virol.	92	1416-1427	2011
Nakayama, E., Tomabechi, D., Matsuno, K., Kishida, N., Yoshida, R., Feldmann, H., and Takada, A.	Antibody-dependent enhancement of Marburg virus infection.	J. Infect. Dis. Suppl	3	S978-985	2011
Ito, K., Igarashi, M., Miyazaki, Y., Murakami, T., Iida, S., Kida, H., and Takada, A.	Gnarled-trunk evolutionary model of influenza A virus hemagglutinin.	PLoS ONE	6	e25953	2011
Aoshi T, Koyama S, Kobiyama K, Akira S, Ishii KJ.	Innate and adaptive immune responses to viral infection and vaccination.	Current Opinion in Virology.	1	226-232	2012
Coban C, Kobiyama K, Aoshi T, Takeshita F, Horii T, Akira S, Ishii KJ.	Novel Strategies to Improve DNA Vaccine Immunogenicity.	Curr Gene Ther.	11	479-484	2011

Ⅳ.　研究成果の刊行物・別刷

JOURNAL OF INTERFERON & CYTOKINE RESEARCH
Volume 31, Number 11, 2011

DOI: 10.1089/jir.2010.0132

Interferon-Inducible Antiviral Protein MxA Enhances Cell Death Triggered by Endoplasmic Reticulum Stress

Akiko Numajiri Haruki,* Tadasuke Naito,* Tomomi Nishie, Shoko Saito, and Kyosuke Nagata

Human myxovirus resistance gene A (MxA) is a type I interferon-inducible protein and exhibits the antiviral activity against a variety of RNA viruses, including influenza virus. Previously, we reported that MxA accelerates cell death of influenza virus-infected cells through caspase-dependent and -independent mechanisms. Similar to other viruses, influenza virus infection induces endoplasmic reticulum (ER) stress, which is one of cell death inducers. Here, we have demonstrated that MxA enhances ER stress signaling in cells infected with influenza virus. ER stress-induced events, such as expression of *BiP* mRNA and processing of *XBP1* mRNA, were upregulated in cells expressing MxA by treatment with an ER stress inducer, tunicamycin (TM), as well as influenza virus infection. TM-induced cell death was also accelerated by MxA. Furthermore, we showed that MxA interacts with BiP and overexpression of BiP reduces MxA-promoted ER stress signaling. Because cell death in virus-infected cells is one of ultimate anti-virus mechanisms, we propose that MxA-enhanced ER stress signaling is a part of the antiviral activity of MxA by accelerating cell death.

Introduction

THE INTERFERON (IFN) SYSTEM plays a central role in host defense against virus infection. IFN-inducible proteins exhibit antiviral roles through translation inhibition, viral RNA metabolism, and so on (García-Sastre and Biron 2006; Sadler and Williams 2008). Furthermore, it was shown that cell death of virus-infected cells, which is one of the ultimate host defense systems, was promoted by some of IFN-inducible proteins, including human myxovirus resistance gene A (MxA) protein (MxA) (Castelli and others 1997; Gil and others 2002; Numajiri and others 2006). MxA is one of the major IFN-inducible proteins and plays a distinct role in the IFN type I-mediated response in cells infected with a variety of viruses such as orthomyxovirus, paramyxovirus, rhabdovirus, togavirus, bunyavirus, coxsackie virus, and hepatitis B virus (Haller and others 2007; Sadler and Williams 2008). A variety of antiviral activities are associated with MxA, although the exact action mechanism is unclear. The anti-viral activity appears to vary depending on the nature of the infecting viruses (Haller and others 2007; Sadler and Williams 2008). MxA may also promote cell death infected with influenza virus (Numajiri and others 2006).

Virus infection causes destruction of infected cells, and induces apoptosis. Most cells undergo cell death while also producing pro-inflammatory cytokines to spread the alarm to their neighboring cells. In turn, viruses employ strategies to regulate the mitochondrial checkpoint for apoptosis, in particular by altering the balance of pro-apoptotic and pro-survival protein levels, by either producing pro-survival inhibitors to lead to cellular death or expressing proteins to maintain cellular survival such as viral Bcl-2 homologs (Galluzzi and others 2008; Postigo and Ferrer 2009).

Several viral proteins have been shown to induce apoptosis through direct effect on mitochondrial compartment or cellular factors. The influenza virus PB1-F2 protein enhances cell death by interaction with ANT3 and VDAC1 proteins at inner and outer mitochondrial membranes, respectively (Zamarin and others 2005). The transforming growth factor-β (TGF-β) activity increases in cells infected with influenza virus. Viral neuraminidase (NA) activates TGF-β, a known inducer of apoptosis, by elimination of sialic acid residues attached to carbohydrates on the latent TGF-β binding protein, which is associated with pro-TGF-β (Schultz-Cherry and Hinshaw 1996; Morris and others 1999). This allows the subsequent removal of the carbohydrate, a pre-determinant for the proteolytic cleavage of pro-TGF-β and release of the active molecule. Viral NS1 and M1 proteins are implicated in modulating apoptotic responses in infected cells. NS1 appears to downregulate apoptosis, although it can induce apoptosis when expressed from a plasmid in absence of virus replication (Morris and others 2002). M1 binds directly with and may inhibit caspase-8 (Zhirnov and others 1999; Timofeeva and others 2001). However, M1 can induce apoptosis in cells expressing this protein from a plasmid. In addition, efficient viral

Department of Infection Biology, Graduate School of Comprehensive Human Sciences, University of Tsukuba, Tsukuba, Japan.
*These two authors contributed to this work equally.

mRNA synthesis has also been shown to be related with apoptosis induction (Stray and Air 2001).

Recently, it was reported that endoplasmic reticulum (ER) stress signaling is triggered and/or regulated by viruses (He 2006). The accumulation of unfolded proteins in the lumen of ER induces a coordinated adaptive program called unfolded protein response (UPR). UPR increases expression of molecular chaperones such as Grp94 and Grp78/BiP to facilitate proper protein folding. Recent studies showed that a variety of viral proteins trigger BiP expression during virus infection, although the effect of upregulation of BiP on virus replication is not fully understood (Jordan and others 2002; Limjindaporn and others 2009). Upon ER stress, activated inositol-requiring enzyme 1 (IRE1) initiates an unconventional splicing of *XBP1* mRNA precursor to excise its unusual intron. The spliced *XBP1* mRNA is efficiently translated into an active basic leucine zipper transcription factor to upregulate transcription of UPR genes (He 2006). Despite of UPR, unfolded proteins often accumulate and can cause apoptosis. C/EBP homologous protein (CHOP), one of the UPR downstream effectors, is a dominant-negative type inhibitor of CCAAT/enhancer-binding proteins. CHOP-mediated apoptosis is known to be coupled with a pathway that suppresses expression of Bcl-2 and intracellular glutathione and the increase of free radicals. The exact downstream target(s) of CHOP remains unclarified (He 2006). It is proposed that IRE1 plays a role in ER stress-mediated apoptosis by the interaction with tumor necrosis factor receptor-associated factor-2, which is thought to be required for the activation of procaspase-12. Activated caspase-12 cleaves procaspase-9 to generate active caspase-9, and consequently leads to activation of the caspase cascade (Urano and others 2000; Rao and others 2002a).

After influenza virus infection, BiP interacts with newly synthesized viral hemagglutinin (HA) and NA proteins (Hurtley and others 1989; Hogue and Nayak 1992). Folding and oligomerization of both proteins are normally efficient, but misfolded HA and NA are generated spontaneously in infected cells, and associate with BiP and then retain in ER. BiP-associated misfolded HA is not transported to the plasma membrane but sustained as complexes in ER for a long period before degradation. These accumulated viral proteins make BiP released from PERK, ATF6, and IRE1, which subsequently activate UPR.

In this study, we have shown that antiviral protein MxA enhances ER stress-mediated cell death after influenza virus infection. Previously, we reported that MxA accelerates cell death induced by influenza viral infection (Mibayashi and others 2002; Numajiri and others 2006). MxA promotes both caspase-dependent and caspase-independent cell death. However, the detailed stimulatory mechanism of cell death induced by MxA is unclear. We found that MxA can enhance transcription of UPR target genes. Furthermore, we have shown that MxA functionally interacts with ER chaperone BiP to promote UPR and apoptosis. Taken altogether, we propose that the cell death promotion activity of MxA plays a role for its antiviral activity.

Materials and Methods

Cells, virus infection, and transfection

Swiss mouse 3T3 cell lines, Swiss3T3-Neo and Swiss3T3-MxA cells (Staeheli and others 1986), were kindly provided by Drs. Haller and Kochs and maintained in Dulbecco's modified Eagle's medium supplemented with 10% fetal bovine serum (FBS). HeLa cells were maintained in minimal essential medium supplemented with 10% FBS. All cells were maintained at 37°C in a 5% CO_2 incubator. For infection, monolayer cultures of Swiss3T3-Neo and Swiss3T3-MxA cells in 100-mm-diameter dishes were washed twice with serum-free medium, and then infected with influenza A/PR/8 virus at a multiplicity of infection (MOI) of 10 plaque forming unit (PFU) per cell. After virus adsorption at 37°C for 1 h, the cells were washed with serum free medium and then incubated with the fresh medium at 37°C for indicated periods. Transfection of HeLa and HEK293T cells with plasmids was carried out by the standard calcium phosphate method or using transfection reagent TransIT (Mirus).

Chemical compounds

Tunicamycin (TM) and salubrinal (Sal) were purchased from Calbiochem. Brefeldin A (BFA) was purchased from Wako. These compounds were dissolved in dimethlysulfoxide.

Construction of plasmid vectors

An eukaryotic expression vector, pCHA-MxA, was constructed previously (Mibayashi and others 2002). To construct pCHA-MxA mutant vectors, pCHA-MxAΔC241 and pCHA-MxAΔC574, the insert cDNAs were amplified by polymerase chain reaction (PCR), digested with *Mlu*I and *Afl*II, and subloned into *Mlu*I- and *Afl*II-digested pCHA vector. PCR amplification was performed using pCHA-MxA as template and primers as follows: 5′-GGACGCGTATGGTTGTTTCCGAA GTGGAC-3′ for pCHA-MxAΔC241 and pCHA-MxAΔC574, 5′-GGCTTAAGTCATTAGACCACCACCAGGCTGAT-3′ for pCHA-MxAΔC241, and 5′-GGCTTAAGTCATTAGGAAGA GTCTGTTGCCGA-3′ for pCHA-MxAΔC574. Plasmids of pCHA-MxAΔC and pCHA-MxAΔN were prepared as described previously (Numajiri and others 2006).

Plasmid vectors for luciferase assays, pGL3-GRP78P(-132)-luc (Yoshida and others 1998) and p5xATF6GL3 (Wang and others 2000) designated ER stress response element (ERSE) and UPR element (UPRE) reporters, respectively, were kind gifts from Drs. Mori and Prywes, respectively. For construction of mammalian expression vector for mouse BiP, a cDNA fragments corresponding to BiP ORF with a FLAG tag at its N-terminus was amplified by reverse transcriptase (RT)-PCR with primers 5′ GCGGATCCCCGCCACCATG ACTACAAGGATGACGACAAGATGATGAAGTTCACTG TGGTGGC 3′ and 5′ GCGGATCCCTACAACTCATCTTT TTCTGATGTATC 3′ and mouse total RNA as template. PCR product was digested with *Bam*HI (TOYOBO), and inserted into the *Bam*HI site of pcDNA3 (Invitrogen) to create pcDNA3-FLAG-BiP. The details for the generation of the plasmid for hNAP-1 (Okuwaki and others 2010) will be described elsewhere.

Reverse transcriptase–polymerase chain reaction

Total RNA was isolated from Swiss3T3-Neo and Swiss3T3-MxA cells by the guanidine method. cDNA was synthesized from total RNA (0.5–2 μg) using Superscript II reverse transcriptase (RT; Invitrogen) and oligo-dT_{20} primer. PCR was performed using the above cDNAs (1/20, vol/vol) as template and a set of specific primers by pre-determined

PCR cycles, under which PCR products are semi-logarithmically amplified. Primer sequences used in this study were as follows: for mouse (m) *BiP*, 5′ AAGGTCTATGAAGGTG AACGACCCC 3′ and 5′ GACCCCAAGACATGTGAGCA ACTGC 3′; for m*XBP1*, 5′ CACGCTTGGGAATGGACACG 3′ and 5′ GATGAGGTCCCCACTGACAG 3′; for m*CHOP*, 5′ GCACGCGTATGGCAGCTGAGTCCCTGC 3′ and 5′ GCG ATATCATGCTTGGTGCAGGCTGA 3′; and for m*β-actin*, 5′ ATGGGTCAGAAGGACTCCTATGTGGG 3′ and 5′ CTAG AAGCACTTGCGGTGCACGATG 3′. The PCR products were separated on 1% agarose gel electrophoresis for *BiP*, *CHOP*, and *β-actin*, and 8% polyacrylamide gel electrophoresis (PAGE) for *XBP1*, and observed by staining with EtBr.

Real-time RT-PCR

Total RNA extraction was performed with RNeasy minikit (Qiagen), and reverse-transcribed into cDNAs by using a ReverTra Ace and oligo(dT) primer (TOYOBO). The amounts of cDNAs for *CHOP* and *β-actin* were quantified using Fast Start SYBR Green Master (Roche).

Trypan blue dye exclusion assay

Typan blue dye exclusion assays were carried out as previously described (Numajiri and others 2006). Swiss3T3-Neo and Swiss3T3-MxA cells in 60-mm-diameter dishes were treated with TM (SIGMA). After cell death induction for indicated periods, both adherent and floating cells were collected together by centrifugation. The cells were resuspend in 0.02% trypan blue (SIGMA) in phosphate-buffered saline (PBS), and dead and living cells were counted using hemocytometer.

Fluorescence-activated cell sorter analysis

Cells were treated as indicated in figure legends, collected, and then stained with propidium iodide (5 μg/mL). Fluorescence-activated cell sorting (FACS) analysis was performed using FACSCalibur instrument (BD biosciences) using CellQuest software.

Luciferase assay

The luciferase activity was determined using commercially available reagents (Promega) according to the manufacturer's protocol. The relative luciferase activity was measured for 10 s with a luminometer. The *Firefly* luciferase activity was normalized as that relative to the *Renilla* luciferase activity derived from a co-transfected control plasmid pRL-SV40 (Promega).

Indirect immunofluorescence assay

The double immunostaining of HA-MxA, FLAG-BiP, and PB1 was carried out at room temperature as follows: HeLa cells grown on glass coverslips in culture dishes were transfected with plasmid DNAs. After 24 h post transfection, the cells were infected with influenza A/PR/8 virus at MOI of 10 PFU per cell according to the protocol described above. After 8 h postinfection (hpi), cells were washed, fixed with PBS containing 4% paraformaldehyde, and then permeabilized with PBS containing 0.5% Triton X-100. The coverslips were soaked in TBS-T [25 mM Tris-HCl (pH 7.9), 137 mM NaCl, and 3 mM KCl, 0.1% Tween 20] containing 5% skim milk for 30 min. Cells were then incubated for 1 h with primary antibodies: mouse anti-HA clone 12CA5 (1:250; Roche), rat anti-HA clone 3F10 (1:3,000; Roche), rabbit anti-PB1 antibodies (1:500) (Naito and others 2007), or mouse anti-FLAG M2 (1:3,000; SIGMA) monoclonal antibodies. After washing with PBS containing 0.1% NP-40, the cells were incubated for 30 min with secondary antibodies: Alexa Fluor 488 goat anti-mouse (1:2,000; Molecular Probe, A11029), Alexa Fluor 568 goat anti-rabbit (1:2,000; Molecular Probe, A11011), and Alexa Fluor 633 goat anti-rat (1:2,000; Molecular Probe, A21094) antibodies. Coverslips were washed with PBS containing 0.1% NP-40, and incubated for 10 min with 10 mM 4′,6′-diamido-2-phenylindole dihydrochloride. After washing with PBS containing 0.1% NP-40, the coverslips were mounted on slide glasses. The cells were then observed under a fluorescence microscope (Carl Zeiss).

Immunoprecipitation assays

Transfected cells were washed with PBS and collected by centrifugation. Cells were re-suspended in IP buffer [20 mM Tris-HCl (pH 7.9), 150 mM NaCl, 30 mM KCl, 1 mM EDTA, and 0.1% NP-40]. After sonication, homogenates were centrifuged at 10,000 rpm at 4°C for 10 min. The supernatant was recovered and used for immunoprecipitation assays. Cell extracts were mixed with mouse anti-MxA KM1124 (Kyowa Medex) or mouse anti-FLAG M2 (SIGMA) antibodies and incubated at 4°C for 2 h. Immunocomplexes were recovered by the addition of protein A Sepharose Fast Flow beads (GE Healthcare). The beads were washed 3 times with IP buffer. Immunoprecipitated proteins were separated by sodium dodecyl sulfate–10% PAGE and subjected to western blot analyses using anti-HA clone 3F10 and anti-FLAG M2 antibodies.

Results

ER stress-mediated cell death is promoted by MxA

Previously, we reported that MxA has the cell death promotion activity (Mibayashi and others 2002; Numajiri and others 2006). After influenza virus infection, cells expressing MxA died faster than MxA-negative cells. Here, we have addressed how the cell death, after influenza virus infection, is triggered in cells expressing MxA. It is well established that one of the triggers of the cell death upon viral infection is the ER stress-induced cell death mechanism (He 2006). Indeed, *BiP* mRNA accumulates after influenza virus infection (Maruoka and others 2003). Thus, we first examined the expression level of *BiP* mRNA in cells expressing MxA upon influenza virus infection. In this study, we used Swiss3T3-MxA, a previously established cell line expressing MxA constitutively (Staeheli and others 1986), because MxA is IFN-inducible in certain cells and the addition of IFN may affect other IFN-related cell death/survival pathways. The level of *BiP* mRNA was upregulated in cells expressing MxA at 3 hpi (Fig. 1A). In addition, splicing of *XBP1* mRNA, an event closely correlated with ER stress, was also enhanced in cells expressing MxA at 3 hpi. These results showed that MxA enhances ER-mediated stress signaling after influenza virus infection.

Next, we examined whether MxA enhances ER stress-mediated stress signaling leading to cell death promotion upon stimuli other than influenza virus infection, because

influenza virus infection may induce a variety of cellular signaling pathways. We utilized an ER stress inducer, TM, which inhibits N-linked glycosylation and thereby causes protein accumulation in ER. Swiss3T3-MxA and Swiss3T3-Neo cells negative in MxA expression were treated with 0.5 μg/mL of TM, and then subjected to trypan blue dye exclusion assays. While TM induces cell death in both MxA-positive and control cells, the number of dead cells was 8–10 times greater in MxA-positive cells (Fig. 1B). More than 70% of MxA-positive cells died at 48 h after TM treatment.

In parallel, we examined whether caspase-12 activation is further enhanced by MxA. Caspase-12 is activated specifically in cells suffered from ER stress (Morishima and others 2002) and functions as the initiator caspase in response to a toxic insult to ER, such as treatment with TM or calcium ionophores (Nakagawa and others 2000). Treatment of cells with TM resulted in the processing of procaspase-12 (48 kDa) (Fig. 1C). We found that the procaspase-12 level decreased, whereas one of cleaved products increased. We could not detect the prodomain, because caspase-12 antibody used (SIGMA; C7611) here does not recognize the prodomain. Key finding is that the cleavage of procaspase-12 was enhanced in MxA-positive cells upon TM treatment. This result suggests that MxA promotes ER stress-mediated cell death after TM treatment.

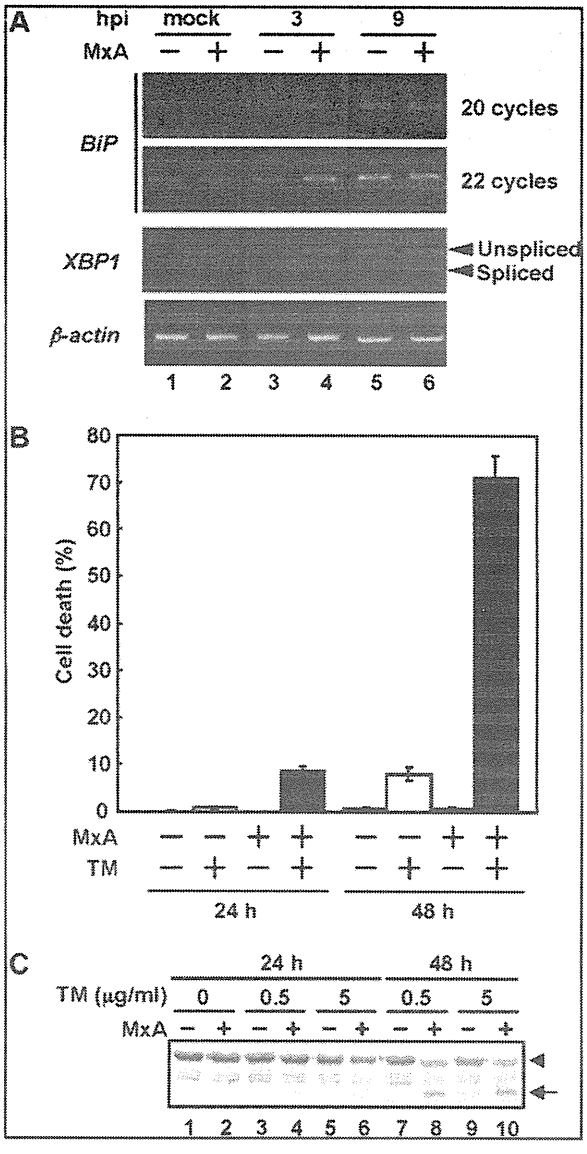

Promotion of apoptosis mediated by MxA is repressed in the presence of a selective inhibitor of ER stress response

MxA was involved in apoptosis acceleration induced by TM (Fig. 1B, C). However, a rapid accumulation of proteins within ER and collapse of Golgi stacks by treatment of TM or BFA may induce various apoptosis pathways beside ER stress-induced cell death. We examined whether MxA specifically functions in UPR-mediated apoptosis by using a selective inhibitor, Sal. Sal blocks dephosphorylation of eukaryotic translation initiation factor 2 subunit α and protects cells from ER stress-induced apoptosis (Boyce and others 2005).

To determine the effect of Sal on ER stress pathway-specific apoptosis acceleration by MxA, we carried out FACS analyses. As shown in Fig. 2A, we confirmed using the FACS method that cell death is induced by TM treatment and further promoted by MxA. Previously, we showed that cell death is enhanced in MxA-expressing cells when cells were treated with cycloheximide (CHX) or ultraviolet irradiation (Numajiri and others 2006). In this report, we examined the impact of Sal on BFA-induced stress condition (Fig. 2B). Cell death was induced by BFA, and enhanced in cells expressing of MxA. Sal suppressed BFA-induced apoptosis, to some extent, not only in MxA-negative cells, but also in MxA-positive cells. These results suggest that apoptosis acceleration by MxA, at least in part, is caused through ER stress signal pathway.

FIG. 1. Cell death is stimulated by TM in cells expressing MxA. **(A)** MxA enhances ER stress caused by influenza virus. Swiss3T3-Neo and Swiss3T3-MxA cells were infected with influenza virus at MOI of 10. After incubation for 3 and 9 h, cells were collected, and the DNA fragment corresponding to *BiP* mRNA was amplified from total RNA by RT-PCR. Resulting products were subjected to 1% agarose gel electrophoresis for *BiP* mRNA (*upper 2 panels*) and *β-actin* mRNA (*lower*) or 8% PAGE for *XBP1* mRNA (*middle*). Unspliced and spliced forms of *XBP1* mRNA were indicated by *arrowheads*. **(B)** Dye exclusion assay. Swiss3T3-Neo (*open columns*) and Swiss3T3-MxA (*filled columns*) cells were treated with TM (0.5 μg/mL). After incubation for 24 and 48 h under cell death induction, cells were collected and subjected to trypan blue dye exclusion assays. **(C)** Cleavage of procaspase-12 upon TM treatment. Swiss3T3-Neo and Swiss3T3-MxA cells were treated with TM (0.5 or 5 μg/mL). After incubation for 24 and 48 h under cell death induction, cells were collected and subjected to western blot analyses with anti-caspase-12 antibody (SIGMA). Procaspase-12 and cleaved forms were indicated by *arrowhead* and *arrow*, respectively. TM, tunicamycin; ER, endoplasmic reticulum; MOI, multiplicity of infection; RT-PCR, reverse transcriptase–polymerase chain reaction.

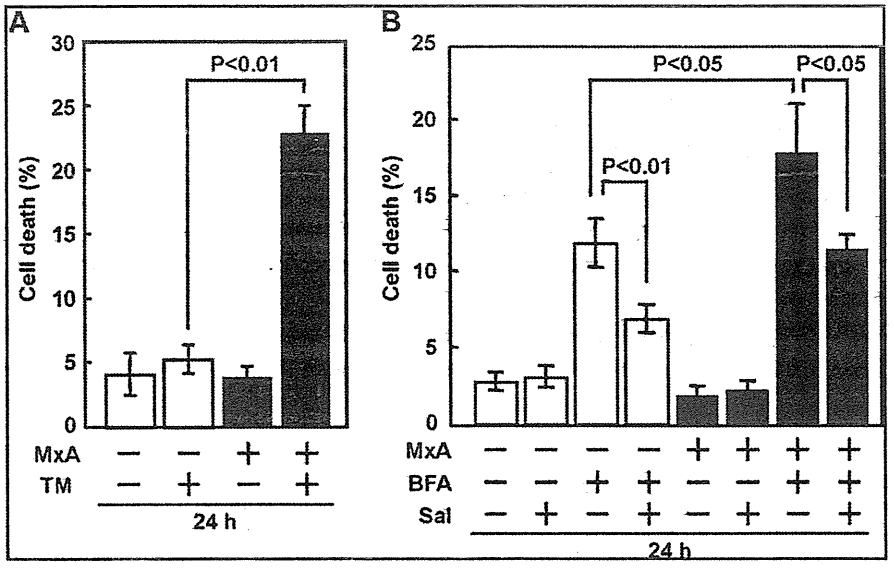

FIG. 2. Sal, a selective ER stress inhibitor suppresses apoptosis accelerated by MxA. **(A)** Swiss3T3-Neo (*open columns*) and Swiss3T3-MxA (*filled columns*) cells were treated with TM (0.5 μg/mL). After incubation for 24 h, cells were collected and subjected to FACS analysis. **(B)** Effect of Sal on MxA-induced cell death. Swiss3T3-Neo (*open columns*) and Swiss3T3-MxA (*filled columns*) cells were treated with 50 μM BFA in the presence or absence of 15 μM Sal. After incubation for 24 h, cells were collected and subjected to FACS analysis. Data were presented as means with standard deviation from 3 independent experiments. FACS, fluorescence-activated cell sorting; BFA, Brefeldin A; Sal, Salubrinal.

MxA accelerates UPR after TM treatment

We next examined whether UPR signaling induced by TM is also enhanced in cells expressing MxA. To this end, we examined the mRNA expression level of genes under the control of the UPR signaling. Swiss3T3-MxA and Swiss3T3-Neo cells were treated with TM, and the mRNA level was examined by RT-PCR method. After 6 and 3 h in the presence of 0.5 and 2.5 μg/mL TM, respectively, the *BiP* mRNA level was increased in cells expressing MxA (Fig. 3A, compare lane 5 with lane 6, and lane 7 with lane 8). From 3 h after treatment with 0.5 μg/mL TM, the spliced form of *XBP1* mRNA was detected in cells expressing MxA, whereas this occurred from 12 h after treatment with TM in MxA-negative cells (Fig. 3B). One of the known signals coordinated with ER stress-induced apoptosis is the expression of CHOP (He 2006). As shown in Fig. 3C, after the treatment with 0.5 μg/mL TM, only MxA-positive cells expressed *CHOP* mRNA. Increase of mRNA amount of the gene under the control of the UPR pathway was distinct only in the presence of low concentrations of TM (Fig. 3C, lanes 4 and 6). This MxA-mediated enhancement was not observed when cells were treated with 2.5 μg/mL TM. MxA may not affect ER signaling induced by vast amounts of unfolded proteins. Furthermore, we confirmed that the amount of *CHOP* mRNA is upregulated in cells transiently expressing MxA (Fig. 3D). Collectively, these suggest that MxA reduces the threshold level of ER stress sensing.

We determined whether MxA enhances the transcription promoter activity directed by ERSE or UPRE under the control of UPR. We utilized pGL3-GRP78P(-132)-luc and p5xATF6GL3 plasmids to monitor ERSE- and UPRE-dependent promoter activities, respectively (Zhu and others 1997; Yoshida and others 1998; Wang and others 2000). As shown in Fig. 3E, F, MxA enhanced both ERSE- and UPRE-dependent promoter activities in response to TM treatment. This enhancement by MxA was in a dose-dependent manner and was undetectable when a reporter plasmid pGL3-GRP78Pmut that lacks ERSE was used (data not shown). These results suggest that MxA affects the signaling pathway leading to the transcription activation upon ER stress response or UPR.

MxA interacts with BiP

We showed that MxA enhances both ATF6- and IRE1-dependent activation of ER stress responses. BiP, an ER chaperone, is known to bind to and stabilize these ER stress sensors (He 2006). Therefore, we consider the possibility that MxA interacts with BiP, either directly or indirectly, and depletes this chaperone in the ER stress response. Since majorities of BiP are localized inside of ER, while MxA is in the cytoplasm, we assumed that an additional factor(s) is involved in the BiP and MxA interaction. However, it is reported that some of BiP is also localized in the cytoplasm (Buchkovich and others 2009). In fact, cytoplasmic BiP interacts with caspase-7 and caspase-12 to prevent cell death (Rao and others 2002b).

As shown in Fig. 4A, MxA and BiP were co-localized around ER in cells co-expressing both proteins. Furthermore, the localization pattern of MxA and BiP in uninfected cells was similar to that observed in influenza virus-infected cells (compare with Fig. 4A, B). At 9 hpi, PB1 was present in the nucleus and the cytoplasm (Fig. 4B). In the same cell, MxA and BiP were co-localized in ER and cytoplasm.

To examine whether MxA interacts with BiP *in vivo*, we performed immunoprecipitation assays using lysates prepared from cells transfected with expression plasmids for FLAG-BiP and either HA-MxA wild type (wt) or mutants (Fig. 4C). Western blot analyses revealed that HA-MxAwt was co-immunoprecipitated with FLAG-BiP when anti-FLAG antibody was used (Fig. 4C, lane 10). We used human nucleosome assembly protein-1-L1 (hNAP-1), one of cytoplasmic proteins, as negative control for overexpression condition (Fig. 4C, lanes 1 and 8). In addition, we tried to identify an interaction domain on MxA and binding specificity with BiP. MxAΔC574 lacking zinc finger motif bound to BiP but only weakly, and MxAΔN interacted with BiP a

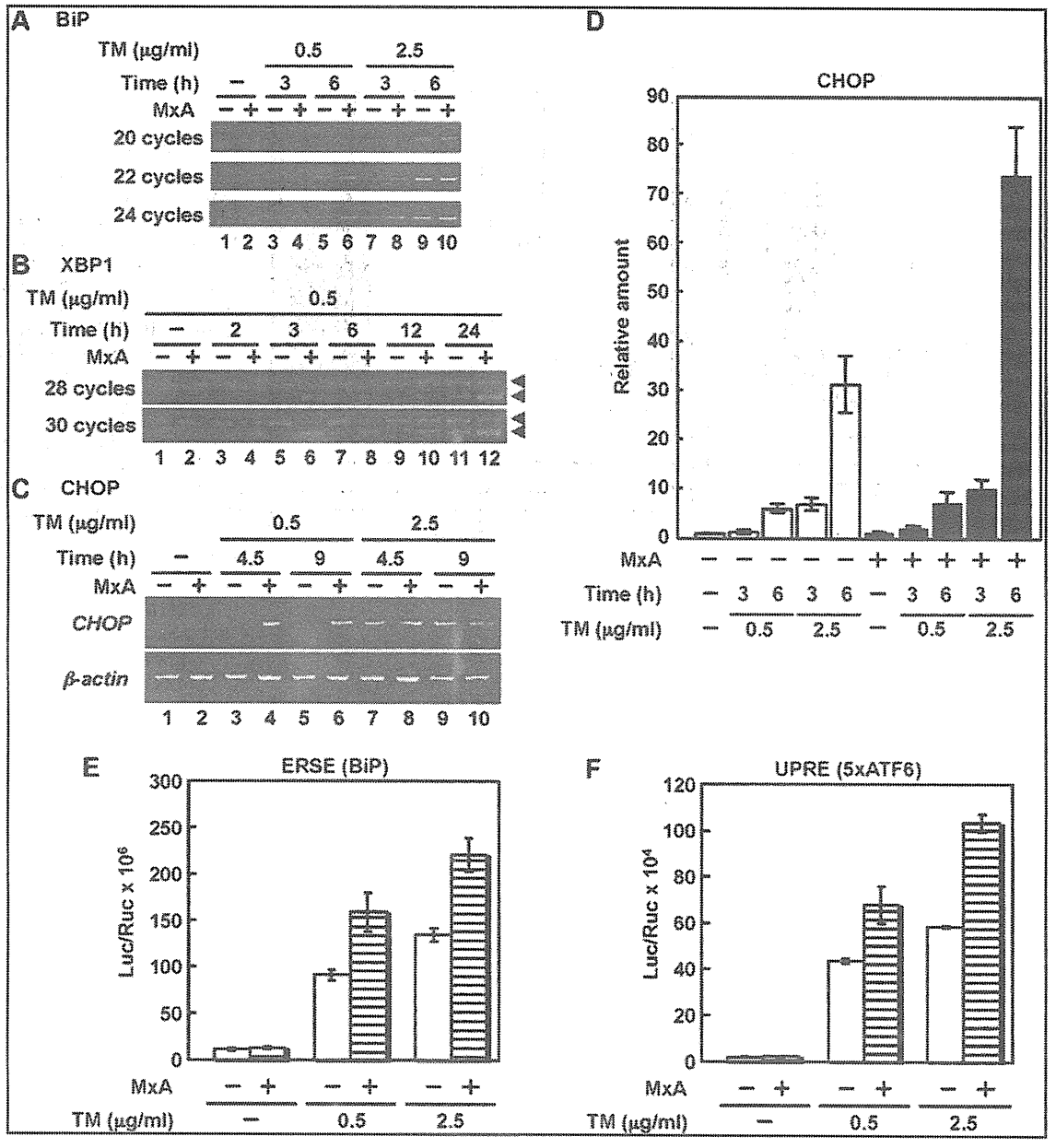

FIG. 3. MxA accelerates UPR after TM treatment. (A–C) Swiss3T3-Neo and Swiss3T3-MxA cells were treated with TM at the indicated concentration. After incubation for indicated time periods, cells were collected, and total RNA were subjected to RT-PCR. Amplified DNA fragments were subjected to separation on 1% agarose gel electrophoresis for *BiP* mRNA (**A**) and *CHOP* mRNA (**C**), or 8% PAGE for *XBP1* mRNA (**B**). Unspliced and spliced forms of *XBP1* mRNA were indicated by *arrowheads*. (**D**) Quantification of *CHOP* mRNA in MxA-transfected cells using real-time RT-PCR. Swiss3T3 cells were transfected with pCHA or pCHA-MxA plasmid with pBabe-puro. At 24 h post transfection, 2 μg/mL puromycin was added, and cells were grown for further 24 h in growth medium in the presence of 2 μg/mL puromycin. Puromycin-resistant cells were treated with TM at indicated concentrations for 3 and 6 h. (**E, F**) MxA enhances both ERSE and UPRE. HeLa cells were transfected with pGL3-GRP78P(-132)-luc or p5xATF6GL3 in the presence (*striped columns*) or absence (*open columns*) of an expression plasmid encoding MxA, pCHA-MxA (Mibayashi and others 2002). pRL-SV40 encoding the *Renilla* luciferase was used for internal control. At 24 h after transfection, the cells were treated with or without TM (0.5 or 2.5 μg/mL) for 12 h, and *Firefly* and *Renilla* luciferase activities were measured. The *Firefly* result was normalized by the *Renilla* luciferase activity. UPR, unfolded protein response; ERSE, ER stress response element; UPRE, UPR element.

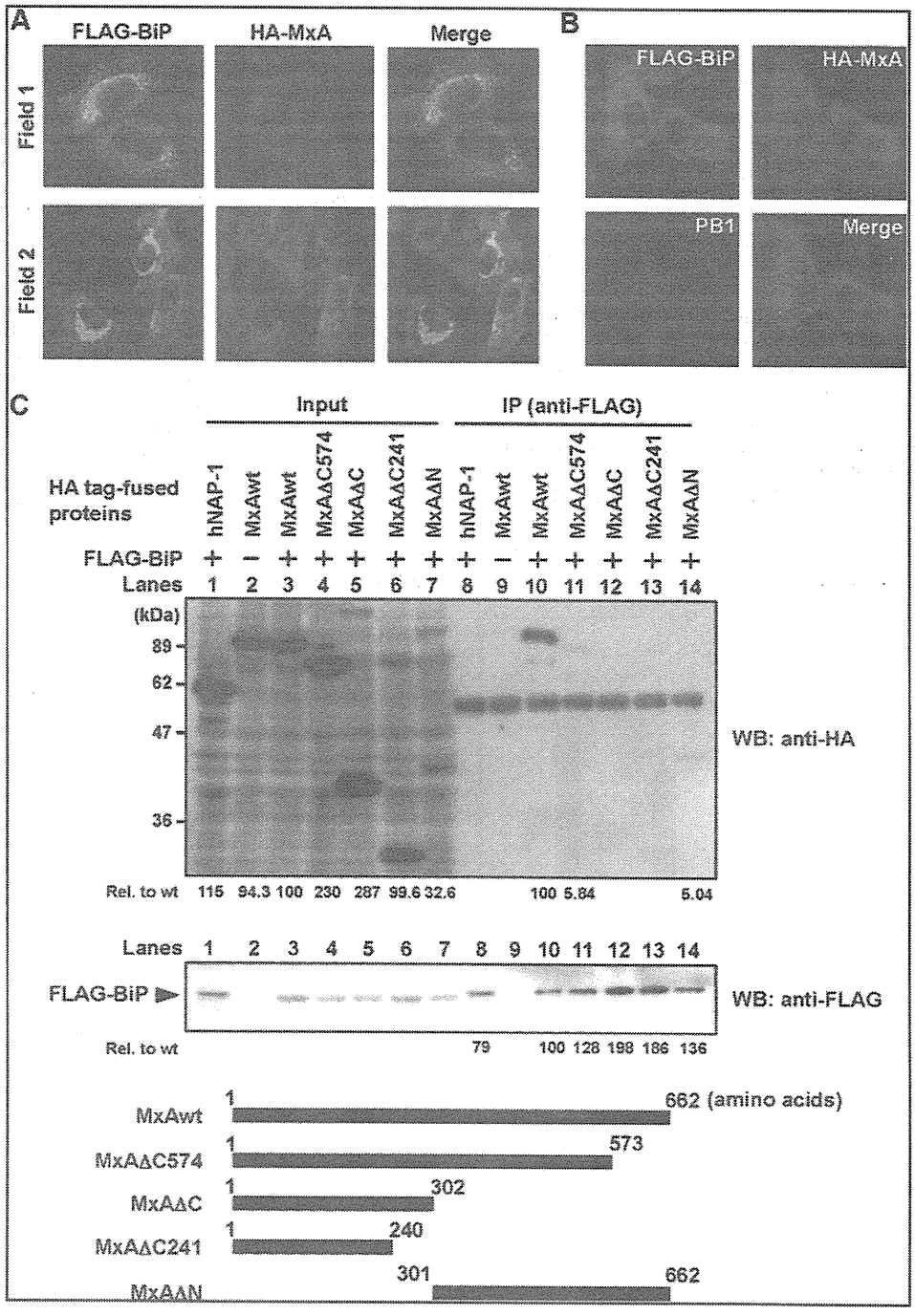

FIG. 4. MxA interacts with BiP. **(A)** Fluorescent immunocytochemical analysis. HeLa cells were transfected with pcDNA-FLAG-BiP and pCHA-MxA, and double-stained with both anti-FLAG and anti-HA antibodies. **(B)** Fluorescent immunocytochemical analysis. HeLa cells were co-transfected with pcDNA3-FLAG-BiP and pCHA-MxA, and at 1 day after transfection, cells were infected with influenza virus at MOI of 10. After incubation for 9 h, cells were collected, and stained with anti-FLAG, anti-HA, and anti-PB1 antibodies. **(C)** Immunoprecipiation assays. HEK293T cells were transfected with pCHA-hNAP-1 (lane 1) or pCHA-MxA mutants (lanes 2–7) in the presence (lanes 1, 3–7) or absence (lane 2) of pcDNA3-FLAG-BiP. Cells were collected at 1 day after transfection, and lysates were subjected to immunoprecipitation assays using anti-FLAG antibody (lanes 8–14). Immunoprecipitated proteins were examined by western blot analyses with anti-HA (*upper panel*) and anti-FLAG antibodies (*lower panel*). Detected protein levels are indicated at the bottom as values relative to those seen in lanes 3 and 10 for the input amount and the immunoprcipitated amount, respectively. MxA mutants used in this assay are schematically illustrated.

little more than MxAΔC574 when compared with the input amounts. However, deletion mutants in the C terminal region, MxAΔC or MxAΔC241 (Fig. 4C, lanes 11 to 14), had virtually no binding capability. Thus, it is quite likely that the region between amino acid positions 301 to 573 of MxA is essential for the binding to BiP. These results indicate that MxA and BiP form a complex around ER. We speculate that this interaction could lead to the activation of ER stress response or the UPR.

BiP suppresses UPR promotion activity of MxA

Finally, we examined whether overexpression of BiP could suppress the ER stress enhancement activity of MxA. We reasoned that either indirect or direct binding of MxA to BiP could be rescued by overexpression of BiP. Reporter gene assays were performed with exogenously overexpressed BiP. Fig. 5A shows that the ER stress response in the absence of TM is not affected by the overexpression of FLAG-BiP. In contrast, in the presence of TM, the activation of ER stress response by MxA was cancelled by overexpressed FLAG-BiP in a dose-dependent manner. Fig. 5B confirmed the expression level of HA-MxA and FLAG-BiP. Thus, it seems likely that ER stress chaperone BiP

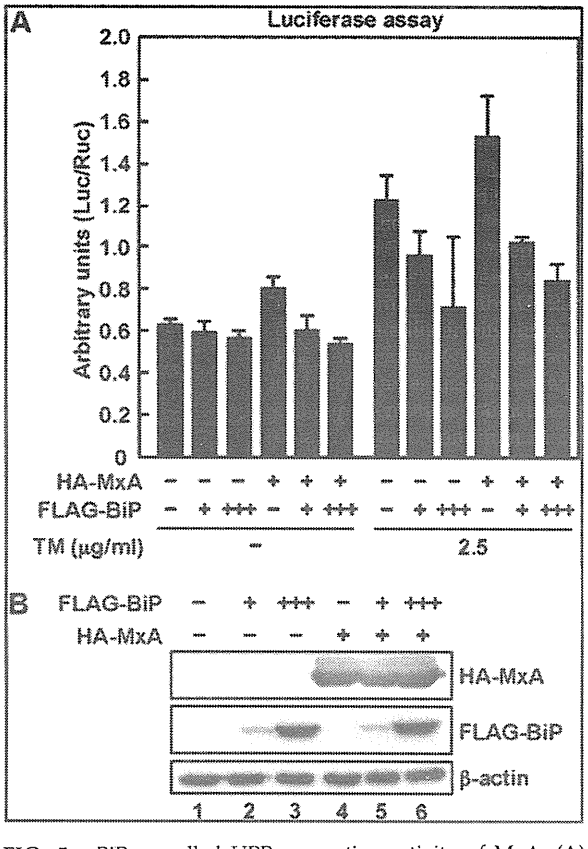

FIG. 5. BiP cancelled UPR promotion activity of MxA. **(A)** Reporter gene assay. HeLa cells were transfected with the reporter plasmid pGL3-GRP78P(-132)-luc with or without pCHA-MxA and pcDNA-FLAG-BiP as described in the figure. At 15 h post transfection, the cells were treated with or without TM (2.5 μg/mL) for 12 h, and the luciferase activity was measured. **(B)** Western blot analyses. Cells treated with TM as shown in **(A)** were subjected to western blot analyses with anti-HA (*upper*), anti-FLAG (*middle*), or anti-β-actin antibodies (*lower*).

cannot be used for its proper role by its depletion through the binding to MxA, either directly or indirectly, on ER membrane. This may reduce the threshold level of ER stress sensing, and thereby promotes the ER stress-induced apoptosis.

Discussion

MxA is an IFN-induced 76 kDa-GTPase that inhibits the multiplication of a variety of RNA viruses, although the exact mechanism of the MxA action is unclear. The antivirus mechanism seems to vary depending on infecting viruses (Schnorr and others 1993; Schneider-Schaulies and others 1994; Landis and others 1998; Gordien and others 2001). When cells expressing MxA are infected with influenza virus, the primary transcription catalyzed by virion-associated viral RNA polymerases occurs at the same level as that in MxA-negative cells (Pavlovic and others 1992). In contrast, viral protein synthesis and genome replication are strongly inhibited (Pavlovic and others 1992). If MxA is forced to be present in the nucleus, nuclear MxA can suppress the influenza virus transcription by interacting with not only the viral polymerase subunit PB2, but also with NP (Turan and others 2004). In addition, we reported that MxA has the cell death promotion activity (Mibayashi and others 2002; Numajiri and others 2006). After influenza virus infection, MxA-positive cells dies faster than MxA-negative cells. We have also shown the caspase-dependent and -independent cell death promotion activity by MxA. It has been reported that the activation of caspase-3 is important during influenza virus proliferation (Queitsch and others 2002). However, the activation level of caspase-3 did not differ between MxA-expressing and MxA-negative cells (Numajiri and others 2006). Therefore, it is possible that MxA could promote cell death without elevation of influenza virus production.

Influenza viruses cause cell death by several mechanisms (Ludwig and others 2006; Sanders and others 2011). Virus infection can induce cell lysis directly, which releases progeny virions and accumulation of a large amount of viral proteins together with potential inflammatory. Promotion of cell death in virus-infected cells may lead to suppression of progeny virion production. The induction of apoptosis might be mediated via intrinsic and/or extrinsic mechanism. It has been shown that viral activation of mitogen-activated protein kinases or their upstream kinases is linked to the onset of apoptosis, and virus infection results in an activation of nuclear factor-κB as an intrinsic pathway. On the other hand, as an extrinsic mechanism of viral apoptosis induction, it has been indicated that the Fas/FasL apoptosis pathway undergoes in a double-stranded RNA activated protein kinase (PKR)-dependent manner in infected cells. The mechanism of viral apoptosis induction might occur via activation of TGF-β, a known apoptosis inducer that is converted from its latent form by NA.

Here, we have addressed the question how MxA promotes cell death after influenza virus infection in light of ER stress signaling. Recent reports suggest that some viruses cause and/or regulate ER stress (Bitko and Barik 2001; Su and others 2002; Tardif and others 2002, 2004; Medigeshi and others 2007). For example, human cytomegalovirus (HCMV) induces splicing of *XBP1* transcript, whereas HCMV suppresses the expression of genes normally regulated by XBP1. It is possible that HCMV utilizes a part of UPR and prevents cell death simultaneously (Isler and others 2005). Dengue

virus envelope protein interacts with BiP and facilitates proper protein folding and protein assembly required for production of progeny virus particles (Limjindaporn and others 2009). In this report, we have shown that MxA enhances ER stress signaling and ER stress-induced cell death upon influenza virus infection. MxA upregulated the transcription level of *BiP* mRNA and the splicing of *XBP1*. MxA also upregulated the transcription level of *CHOP* gene, which is known to be a key mediator for ER stress-induced cell death. Consistent with our findings, CHOP-dependent premature cell death may represent a host defense mechanism to limit viral replication (Medigeshi and others 2007). Previously, we reported that the cell death promotion activity was detected for both MxAwt and MxAΔN, but not for MxΔC in cells treated with CHX as stress inducer. Here, we have shown that the C terminal region on MxA containing oligomelization domain was important in the interaction with BiP. Therefore, similar to the promotion of CHX-induced cell death by MxA, MxA may function as apoptosis accelerator for ER stress-mediated cell death through the same C terminal region.

Previous studies demonstrated that a portion of MxA is localized at membranes belonging to the COP-I-positive subdomain of the smooth ER-Golgi-intermediate compartment (Accola and others 2002; Stertz and others 2006). Furthermore, it has been reported that binding of MxA to viral nucleocapsid protein of La Crosse virus occurs on membranes of the smooth ER-Golgi boundary region and lead to a depletion of the nucleocapsid protein from the viral replication sites (Kochs and others 2002). However, it is presently not clear how MxA interacts with lipid membranes. Anchoring of MxA to distinct membrane compartments may influence the antiviral activity and/or specificity. Recently, Gao and others (2010) reported that the crystal structure of oligomerized stalk region of MxA, which is composed of the middle domain and the GTPase effector domain. The MxA could form a linear oligomers comprised of 13 to 14 dimers. It is not clear how a huge complex of MxA formed through this structure is associated with or incorporated into intracellular membranes. Further studies are needed to clarify details of the connection of MxA-mediated ER stress promotion with antiviral activity.

Acknowledgments

We thank Drs. O. Haller and P. Staeheli (University of Freiburg, Freiburg, Germany), K. Mori (Kyoto University, Kyoto, Japan), and R. Prywes (Columbia University, New York) for their generous gifts of Swiss3T3 and Swiss3T3-MxA cells, and MxA wild-type cDNA, pGL3-GRP78P(-132)-luc, and p5xATF6GL3, respectively. We also thank Dr. Kiong Ho for proofreading the article. This work was supported in part by grants-in-aid from the Ministry of Education, Culture, Sports, Science, and Technology of Japan (T.N. and K.N.).

Author Disclosure Statement

No competing financial interests exist.

References

Accola M, Huang B, Al Masri A, McNiven M. 2002. The antiviral dynamin family member, MxA, tubulates lipids and localizes to the smooth endoplasmic reticulum. J Biol Chem 277:21829–21835.

Bitko V, Barik S. 2001. An endoplasmic reticulum-specific stress-activated caspase (caspase-12) is implicated in the apoptosis of A549 epithelial cells by respiratory syncytial virus. J Cell Biochem 80:441–454.

Boyce M, Bryant KF, Jousse C, Long K, Harding HP, Scheuner D, Kaufman RJ, Ma D, Coen DM, Ron D, Yuan J. 2005. A selective inhibitor of eIF2alpha dephosphorylation protects cells from ER stress. Science 307:935–939.

Buchkovich N, Maguire T, Paton A, Paton J, Alwine J. 2009. The endoplasmic reticulum chaperone BiP/GRP78 is important in the structure and function of the human cytomegalovirus assembly compartment. J Virol 83:11421–11428.

Castelli J, Hassel B, Wood K, Li X, Amemiya K, Dalakas M, Torrence P, Youle R. 1997. A study of the interferon antiviral mechanism: apoptosis activation by the 2-5A system. J Exp Med 186:967–972.

Galluzzi L, Brenner C, Morselli E, Touat Z, Kroemer G. 2008. Viral control of mitochondrial apoptosis. PLoS Pathog 4, e1000018.

Gao S, von der Malsburg A, Paeschke S, Behlke J, Haller O, Kochs G, Daumke O. 2010. Structural basis of oligomerization in the stalk region of dynamin-like MxA. Nature 465:502–506.

García-Sastre A, Biron C. 2006. Type 1 interferons and the virus-host relationship: a lesson in détente. Science 312:879–882.

Gil J, García M, Esteban M. 2002. Caspase 9 activation by the dsRNA-dependent protein kinase, PKR: molecular mechanism and relevance. FEBS Lett 529:249–255.

Gordien E, Rosmorduc O, Peltekian C, Garreau F, Bréchot C, Kremsdorf D. 2001. Inhibition of hepatitis B virus replication by the interferon-inducible MxA protein. J Virol 75:2684–2691.

Haller O, Staeheli P, Kochs G. 2007. Interferon-induced Mx proteins in antiviral host defense. Biochimie 89:812–818.

He B. 2006. Viruses, endoplasmic reticulum stress, and interferon responses. Cell Death Differ 13:393–403.

Hogue BG, Nayak DP. 1992. Synthesis and processing of the influenza virus neuraminidase, a type II transmembrane glycoprotein. Virology 188:510–517.

Hurtley SM, Bole DG, Hoover-Litty H, Helenius A, Copeland CS. 1989. Interactions of misfolded influenza virus hemagglutinin with binding protein (BiP). J Cell Biol 108:2117–2126.

Isler J, Skalet A, Alwine J. 2005. Human cytomegalovirus infection activates and regulates the unfolded protein response. J Virol 79:6890–6899.

Jordan R, Wang L, Graczyk T, Block T, Romano P. 2002. Replication of a cytopathic strain of bovine viral diarrhea virus activates PERK and induces endoplasmic reticulum stress-mediated apoptosis of MDBK cells. J Virol 76:9588–9599.

Kochs G, Janzen C, Hohenberg H, Haller O. 2002. Antivirally active MxA protein sequesters La Crosse virus nucleocapsid protein into perinuclear complexes. Proc Natl Acad Sci U S A 99:3153–3158.

Landis H, Simon-Jödicke A, Klöti A, Di Paolo C, Schnorr J, Schneider-Schaulies S, Hefti H, Pavlovic J. 1998. Human MxA protein confers resistance to Semliki Forest virus and inhibits the amplification of a Semliki Forest virus-based replicon in the absence of viral structural proteins. J Virol 72:1516–1522.

Limjindaporn T, Wongwiwat W, Noisakran S, Srisawat C, Netsawang J, Puttikhunt C, Kasinrerk W, Avirutnan P, Thiemmeca S, Sriburi R, Sittisombut N, Malasit P, Yenchitsomanus P. 2009. Interaction of dengue virus envelope protein with endoplasmic reticulum-resident chaperones facilitates dengue virus production. Biochem Biophys Res Commun 379:196–200.

Ludwig S, Pleschka S, Planz O, Wolff T. 2006. Ringing the alarm bells: signalling and apoptosis in influenza virus infected cells. Cell Microbiol 8:375–386.

Maruoka S, Hashimoto S, Gon Y, Nishitoh H, Takeshita I, Asai Y, Mizumura K, Shimizu K, Ichijo H, Horie T. 2003. ASK1 regulates influenza virus infection-induced apoptotic cell death. Biochem Biophys Res Commun 307:870–876.

Medigeshi G, Lancaster A, Hirsch A, Briese T, Lipkin W, Defilippis V, Früh K, Mason P, Nikolich-Zugich J, Nelson J. 2007. West Nile virus infection activates the unfolded protein response, leading to CHOP induction and apoptosis. J Virol 81:10849–10860.

Mibayashi M, Nakad K, Nagata K. 2002. Promoted cell death of cells expressing human MxA by influenza virus infection. Microbiol Immunol 46:29–36.

Morishima N, Nakanishi K, Takenouchi H, Shibata T, Yasuhiko Y. 2002. An endoplasmic reticulum stress-specific caspase cascade in apoptosis. Cytochrome c-independent activation of caspase-9 by caspase-12. J Biol Chem 277:34287–34294.

Morris SJ, Price GE, Barnett JM, Hiscox SA, Smith H, Sweet C. 1999. Role of neuraminidase in influenza virus-induced apoptosis. J Gen Virol 80 (Pt 1):137–146.

Morris SJ, Smith H, Sweet C. 2002. Exploitation of the Herpes simplex virus translocating protein VP22 to carry influenza virus proteins into cells for studies of apoptosis: direct confirmation that neuraminidase induces apoptosis and indications that other proteins may have a role. Arch Virol 147:961–979.

Naito T, Momose F, Kawaguchi A, Nagata K. 2007. Involvement of Hsp90 in assembly and nuclear import of influenza virus RNA polymerase subunits. J Virol 81:1339–1349.

Nakagawa T, Zhu H, Morishima N, Li E, Xu J, Yankner B, Yuan J. 2000. Caspase-12 mediates endoplasmic-reticulum-specific apoptosis and cytotoxicity by amyloid-beta. Nature 403:98–103.

Numajiri A, Mibayashi M, Nagata K. 2006. Stimulus-dependent and domain-dependent cell death acceleration by an IFN-inducible protein, human MxA. J Interferon Cytokine Res 26: 214–219.

Okuwaki M, Kato K, Nagata K. 2010. Functional characterization of human nucleosome assembly protein 1-like proteins as histone chaperones. Genes Cells 15:13–27.

Pavlovic J, Haller O, Staeheli P. 1992. Human and mouse Mx proteins inhibit different steps of the influenza virus multiplication cycle. J Virol 66:2564–2569.

Postigo A, Ferrer P. 2009. Viral inhibitors reveal overlapping themes in regulation of cell death and innate immunity. Microbes Infect 11:1071–1078.

Queitsch C, Sangster TA, Lindquist S. 2002. Hsp90 as a capacitor of phenotypic variation. Nature 417:618–624.

Rao R, Castro-Obregon S, Frankowski H, Schuler M, Stoka V, del Rio G, Bredesen D, Ellerby H. 2002a. Coupling endoplasmic reticulum stress to the cell death program. An Apaf-1-independent intrinsic pathway. J Biol Chem 277:21836–21842.

Rao R, Peel A, Logvinova A, del Rio G, Hermel E, Yokota T, Goldsmith P, Ellerby L, Ellerby H, Bredesen D. 2002b. Coupling endoplasmic reticulum stress to the cell death program: role of the ER chaperone GRP78. FEBS Lett 514:122–128.

Sadler A, Williams B. 2008. Interferon-inducible antiviral effectors. Nat Rev Immunol 8:559–568.

Sanders CJ, Doherty PC, Thomas PG. 2011. Respiratory epithelial cells in innate immunity to influenza virus infection. Cell Tissue Res 343:13–21.

Schneider-Schaulies S, Schneider-Schaulies J, Schuster A, Bayer M, Pavlovic J, ter Meulen V. 1994. Cell type-specific MxA-mediated inhibition of measles virus transcription in human brain cells. J Virol 68:6910–6917.

Schnorr J, Schneider-Schaulies S, Simon-Jödicke A, Pavlovic J, Horisberger M, ter Meulen V. 1993. MxA-dependent inhibition of measles virus glycoprotein synthesis in a stably transfected human monocytic cell line. J Virol 67:4760–4768.

Schultz-Cherry S, Hinshaw VS. 1996. Influenza virus neuraminidase activates latent transforming growth factor beta. J Virol 70:8624–8629.

Staeheli P, Haller O, Boll W, Lindenmann J, Weissmann C. 1986. Mx protein: constitutive expression in 3T3 cells transformed with cloned Mx cDNA confers selective resistance to influenza virus. Cell 44:147–158.

Stertz S, Reichelt M, Krijnse-Locker J, Mackenzie J, Simpson J, Haller O, Kochs G. 2006. Interferon-induced, antiviral human MxA protein localizes to a distinct subcompartment of the smooth endoplasmic reticulum. J Interferon Cytokine Res 26:650–660.

Stray SJ, Air GM. 2001. Apoptosis by influenza viruses correlates with efficiency of viral mRNA synthesis. Virus Res 77:3–17.

Su H, Liao C, Lin Y. 2002. Japanese encephalitis virus infection initiates endoplasmic reticulum stress and an unfolded protein response. J Virol 76:4162–4171.

Tardif K, Mori K, Kaufman R, Siddiqui A. 2004. Hepatitis C virus suppresses the IRE1-XBP1 pathway of the unfolded protein response. J Biol Chem 279:17158–17164.

Tardif K, Mori K, Siddiqui A. 2002. Hepatitis C virus subgenomic replicons induce endoplasmic reticulum stress activating an intracellular signaling pathway. J Virol 76:7453–7459.

Timofeeva TA, Klenk ND, Zhirnov OP. 2001. [Identification of the protease-binding domain in the N-terminal region of the influenza A virus matrix protein M1]. Mol Biol (Mosk) 35:484–491.

Turan K, Mibayashi M, Sugiyama K, Saito S, Numajiri A, Nagata K. 2004. Nuclear MxA proteins form a complex with influenza virus NP and inhibit the transcription of the engineered influenza virus genome. Nucleic Acids Res 32:643–652.

Urano F, Wang X, Bertolotti A, Zhang Y, Chung P, Harding H, Ron D. 2000. Coupling of stress in the ER to activation of JNK protein kinases by transmembrane protein kinase IRE1. Science 287:664–666.

Wang Y, Shen J, Arenzana N, Tirasophon W, Kaufman R, Prywes R. 2000. Activation of ATF6 and an ATF6 DNA binding site by the endoplasmic reticulum stress response. J Biol Chem 275:27013–27020.

Yoshida H, Haze K, Yanagi H, Yura T, Mori K. 1998. Identification of the cis-acting endoplasmic reticulum stress response element responsible for transcriptional induction of mammalian glucose-regulated proteins. Involvement of basic leucine zipper transcription factors. J Biol Chem 273:33741–33749.

Zamarin D, García-Sastre A, Xiao X, Wang R, Palese P. 2005. Influenza virus PB1-F2 protein induces cell death through mitochondrial ANT3 and VDAC1. PLoS Pathog 1:e4.

Zhirnov OP, Konakova TE, Garten W, Klenk H. 1999. Caspase-dependent N-terminal cleavage of influenza virus nucleocapsid protein in infected cells. J Virol 73:10158–10163.

Zhu C, Johansen F, Prywes R. 1997. Interaction of ATF6 and serum response factor. Mol Cell Biol 17:4957–4966.

Address correspondence to:
Prof. Kyosuke Nagata
Department of Infection Biology
Graduate School of Comprehensive Human Sciences
University of Tsukuba
1-1-1 Tennodai
Tsukuba 305-8575
Japan

E-mail: knagata@md.tsukuba.ac.jp

Received 28 September 2010/Accepted 5 July 2011

JOURNAL OF VIROLOGY, Aug. 2011, p. 7504–7512 Vol. 85, No. 15
0022-538X/11/$12.00 doi:10.1128/JVI.02375-10

Recognition of Cap Structure by Influenza B Virus RNA Polymerase Is Less Dependent on the Methyl Residue than Recognition by Influenza A Virus Polymerase▽†

Chitose Wakai,[1,2] Minako Iwama,[2] Kiyohisa Mizumoto,[2,3] and Kyosuke Nagata[1]*

Department of Infection Biology, Graduate School of Comprehensive Human Sciences, University of Tsukuba, 1-1-1 Tennodai, Tsukuba 305-8575, Japan[1]; Department of Biochemistry, School of Pharmaceutical Sciences, Kitasato University, 5-9-1 Shirokane, Minato-ku, Tokyo 108-8641, Japan[2]; and Microbial Chemistry Research Center, 3-14-23 Kamiosaki, Shinagawa-ku, Tokyo 141-0021, Japan[3]

Received 12 November 2010/Accepted 10 May 2011

The cap-dependent endonuclease activity of the influenza virus RNA-dependent RNA polymerase cleaves host mRNAs to produce capped RNA fragments for primers to initiate viral mRNA synthesis. The influenza A virus (FluA) cap-dependent endonuclease preferentially recognizes the cap1 structure (m^7GpppNm). However, little is known about the substrate specificity of the influenza B virus (FluB) endonuclease. Here, we determined the substrate specificity of the FluB polymerase using purified viral RNPs and ^{32}P-labeled polyribonucleotides containing a variety of cap structures (m^7GpppGm, m^7GpppG, and GpppG). We found that the FluA polymerase cleaves m^7G-capped RNAs preferentially. In contrast, the FluB polymerase could efficiently cleave not only m^7G-capped RNAs but also unmethylated GpppG-RNAs. To identify a key amino acid(s) related to the cap recognition specificity of the PB2 subunit, the transcription activity of FluB polymerases containing mutated cap-binding domains was examined by use of a minireplicon assay system. In the case of FluA PB2, Phe323, His357, and Phe404, which stack the m^7GTP, and Glu361 and Lys376, which make hydrogen bonds with a guanine base, were essential for the transcription activity. In contrast, in the case of FluB PB2, the stacking interaction of Trp359 with a guanine base and putative hydrogen bonds using Gln325 and Glu363 were enough for the transcription activity. Taking these results together with the result for the cap-binding activity, we propose that the cap recognition pocket of FluB PB2 does not have the specificity for m^7G-cap structures and thus is more flexible to accept various cap structures than FluA PB2.

Influenza A virus (FluA) and influenza B virus (FluB) belong to the family of *Orthomyxoviridae*. The genomes of FluA and FluB are composed of a set of eight segments of RNA (vRNA) of negative polarity. vRNA is complexed with nucleoprotein (NP) and associated with the RNA polymerase to form viral ribonucleoprotein (vRNP) complexes. vRNP is an essential unit for both transcription and replication (9). In transcription, the RNA polymerase catalyzes not only RNA polymerization and polyadenylation of mRNA but also cleavage of host mRNAs to generate capped RNA fragments. The RNA polymerase is composed of one molecule each of three viral proteins, PB1, PB2, and PA. PB1 plays central roles in both RNA polymerase assembly (27, 31) and RNA polymerization (6). It contains the conserved motifs characteristic of RNA-dependent RNA polymerases and is directly involved in RNA chain elongation (1, 2). It binds to 5′- and 3′-terminal sequences of vRNA and cRNA (cRNA to vRNA), which are conserved in all segments and act as *cis*-acting elements for the viral RNA synthesis. PB2 is required for transcription and binds to the cap structures of host mRNAs. Recently, the structural features of the cap-binding site in FluA PB2 and the FluA PB1-PB2 contact site have been determined by functional studies and crystallography (12, 31). PA is involved in not only virus genome replication but also transcription as an endonuclease for generation of primers for RNA synthesis (8, 10, 13, 19, 36). It is also reported that PA is important for the polymerase assembly (19). The structure of the PB1-PA contact site has also been determined crystallographically (14, 27).

The FluA polymerase exhibits a cap-dependent endonuclease activity, which cleaves host mRNAs to produce capped RNA fragments with lengths of 11 to 13 nucleotides (nt). The resulting capped RNA fragment serves as a primer to initiate viral mRNA synthesis. It is well known that in the case of the FluA polymerase, eukaryotic mRNAs containing m^7G(5′)ppp(5′)Nm (cap1) and m^7G(5′)ppp(5′)NmN′m (cap2) structures stimulate *in vitro* viral RNA transcription strongly (4, 5, 29). Removal of m^7G of the cap from mRNA eliminates the priming activity, and naturally occurring uncapped mRNAs do not prime transcription (5, 29). In addition, the presence of methyl groups in the cap is required for the priming activity; reovirus mRNAs with 5′-terminal GpppG are inactive as primers (3). It has also been demonstrated that each of the two methyl groups in the cap1 structure, the 7-methyl residue of guanine and the 2′-*O*-methyl on the ribose of guanosine, strongly influences the capped RNA-primed transcription activity (4).

Biochemical and structural studies revealed the functional structures of the cap-binding proteins, including FluA PB2 (12), human translation initiation factor 4E (eIF4E) (33, 34),

* Corresponding author. Mailing address: Department of Infection Biology, Graduate School of Comprehensive Human Sciences, University of Tsukuba, 1-1-1 Tennodai, Tsukuba 305-8575, Japan. Phone and fax: 81-29-853-3233. E-mail: knagata@md.tsukuba.ac.jp.

† Supplemental material for this article may be found at http://jvi.asm.org/.

▽ Published ahead of print on 18 May 2011.

human nuclear cap-binding protein 20 (CBP20) (23), and vaccinia virus (nucleoside-2′-*O*-)-methyltransferase (VP39) (16). The overall structures of these four cap-binding proteins differ widely due to their evolutionarily unrelated origins, but the cap-binding pockets form a common structure and preferentially bind to the 7-methylated cap structure. These cap-binding proteins hardly bind to the unmethylated cap structure.

Most of our knowledge on the transcription mechanism of the influenza virus genome has been derived from studies on the FluA polymerase, whereas little is known about the FluB polymerase. It is reported that α-amanitin, a potent inhibitor for the host cell RNA polymerase II, inhibits influenza virus transcription, suggesting that eukaryotic mRNAs containing the cap structure are essential for influenza virus transcription (21). Using α-amanitin, we found that the growth of FluB is more sensitive to the amount of cellular mRNA than that of FluA (data not shown). To elucidate the transcription initiation mechanism of the FluB polymerase, we tried to determine the specificity of cap recognition by the FluB polymerase. First, we compared the substrate specificities of FluA and FluB polymerases using purified vRNPs and various capped RNA substrates (m^7GpppGm-, m^7GpppG-, and GpppG-RNA) and found that the FluB polymerase efficiently cleaves not only m^7G-capped RNAs but also unmethylated GpppG-RNA, whereas the FluA polymerase cleaves m^7G-capped RNAs specifically. We then tried to identify key amino acids related to the cap recognition of FluB PB2. In order to examine the transcription activity using mutated PB2 proteins, we utilized FluA and FluB minireplicon assay systems using a virus polymerase-dependent reporter gene (17, 35). The minireplicon system has been utilized for a number of functional analyses of *cis*-acting elements with the viral genome and *trans*-acting viral factors (10, 35). The reporter gene contains a coding region flanked by each viral 5′ and 3′ untranslated region (UTR), which function as promoters, and therefore mimics an influenza virus genomic segment. Using this assay system, we identified the important amino acids required for the cap recognition by the FluB polymerase by referencing functionally important amino acids in the FluA polymerase (12).

Based on the findings using the assay systems, we propose that the FluB polymerase possesses a novel cap recognition mechanism, which is different not only from the FluA polymerase but also from well-known cap-binding proteins. These findings could be important to develop novel anti-influenza virus drugs targeting the cap recognition and cleavage reaction.

MATERIALS AND METHODS

Biological materials. Monolayer cultures of 293T and MDCK cells were maintained at 37°C in Dulbecco's modified Eagle medium (DMEM) and minimal essential medium (MEM) (Nissui), respectively, supplemented with 10% fetal calf serum (Cell Culture Technologies). Influenza virus A/Panama/2007/99 (A/PA/99) and B/Shanghai/361/2002 (B/SH/02) were kindly supplied by Y. Suzuki and T. Gotanda (Kitasato Institute, Research Center for Biologicals, Saitama, Japan). Vaccinia virus capping enzyme and recombinant human mRNA (guanine-7-)methyltransferase (rhMTase) were prepared according to a previously described procedure (28).

Cloning of cDNAs for viral RNA polymerase subunits and nucleoprotein cDNA. For construction of mammalian expression vectors for influenza virus polymerase subunits (PB1, PB2, and PA) and nucleoprotein (NP), cDNAs corresponding to the full-length PB1, PB2 with a FLAG tag at its C terminus (PB2cFLAG), PA, and NP were amplified by reverse transcription-PCR (RT-PCR) from vRNAs of influenza virus A/PA/99 and B/SH/02 as templates using the following sets of phosphorylated primers (see Table S1 in the supplemental material): A-PB1-FOR and A-PB1-REV for FluA-PB1, A-PB2-FOR and A-PB2-cFLAG-REV for FluA-PB2cFLAG, A-PA-FOR and A-PA-REV for FluA-PA, A-NP-FOR and A-NP-REV for FluA-NP, B-PB1-FOR and B-PB1-REV for FluB-PB1, B-PB2-FOR and B-PB2-cFLAG-REV for FluB-PB2cFLAG, B-PA-FOR and B-PA-REV for FluB-PA, and B-NP-FOR and B-NP-REV for FluB-NP. The PCR products were then cloned into the EcoRV site of pCAGGS-P7 (7), resulting in construction of pCAGGS-Panama-PB1, pCAGGS-Panama-PB2-cFLAG, pCAGGS-Panama-PA, pCAGGS-Panama-NP, pCAGGS-Shanghai-PB1, pCAGGS-Shanghai-PB2-cFLAG, pCAGGS-Shanghai-PA, and pCAGGS-Shanghai-NP. cDNAs for PB2 mutants were prepared by site-directed mutagenesis using the primer sets for FluA-PB2-cFLAG and FluB-PB2-cFLAG and mutant primer sets (see Table S2 in the supplemental material). The PB2 mutant genes have been fully sequenced by standard methods (35).

Preparation of influenza virus vRNP. To prepare vRNP, we first treated purified influenza virus virions at 30°C for 60 min with a disruption buffer consisting of 50 mM Tris-HCl (pH 8.0), 100 mM KCl, 5 mM $MgCl_2$, 1 mM dithiothreitol (DTT), 5% glycerol, 2% Triton X-100, and 2% lysolecithin according to a method described previously (32). The sample was then directly subjected to centrifugation on a 30 to 60% (wt/vol) linear gradient of glycerol on a 70% (wt/vol) glycerol cushion in 50 mM Tris-HCl (pH 8.0) and 150 mM NaCl in a Beckman MLS-50 rotor with adapters at 163,000 × g_{AV} for 3 h at 4°C. Fractionation was carried out from the top of the gradient. Fractions containing vRNP were pooled and then used for *in vitro* endonuclease and elongation assays.

Preparation of various RNA substrates. Triphosphate-ended RNA with the 33-nucleotide sequence 5′-GAAAAAAAAAAAAAAAAAAAAAAAAAAAAAAUAAA-3′, designated pppG-RNA, was synthesized by using T7 RNA polymerase (Amersham Biosciences) and a synthetic DNA template. The protocol was previously described (30). Briefly, to prepare the template for the T7 RNA polymerase, the oligonucleotide T7P (5′-TAATACGACTCACTATA-3′), corresponding to the T7 promoter (−17 to −1), was annealed to the template oligonucleotide T7-polyA-R1 (5′-TTTATTTTTTTTTTTTTTTTTTTTTTTTTTTCTATAGTGAGTCGTATTA-3′, where the underlined sequence is complementary to the T7 promoter [−17 to −1]). After the transcription reaction, the transcription mixture was treated with DNase I (Roche Applied Science). RNA was then extracted with phenol-chloroform, ethanol precipitated, and used as a capping substrate. To synthesize $m^7G[^{32}P]$pppGm-RNA and $G[^{32}P]$pppG-RNA, 50 pmol of pppG-RNA was incubated at 37°C for 2 h in the presence of 8 μM [α-^{32}P]GTP (800 cpm/fmol) and an appropriate amount of purified vaccinia virus capping enzyme, which has guanylyltransferase, guanine-7-methyltransferase, and ribose-2′-*O*-methyl-transferase activities, in a reaction mixture (50 μl) containing 50 mM Tris-HCl (pH 7.9), 2 mM $MgCl_2$, 40 mM NaCl, and 20 mM DTT in the presence or absence of 150 μM *S*-adenosyl-L-methionine (AdoMet). After the reaction, capped RNA was extracted with phenol-chloroform, ethanol precipitated, and dissolved in H_2O. To synthesize $m^7G[^{32}P]$pppG-RNA, 0.4 pmol of $G[^{32}P]$pppG-RNA was incubated at 30°C for 20 min with 15 ng/μl of rhMTase in a reaction mixture (20 μl) containing 25 mM Tris-HCl (pH 7.9), 0.5 mM DTT, 0.1 mg/ml bovine serum albumin (BSA), and 50 μM AdoMet. The RNA was extracted with phenol-chloroform, ethanol precipitated, and dissolved in H_2O. To confirm the cap structure on the synthesized RNA, the cap structure of the synthesized ^{32}P-capped RNA was liberated by digestion with nuclease P_1 (Wako) (28). The reaction product was analyzed by thin-layer chromatography (TLC) on a polyethyleneimine (PEI)-cellulose plate (PEI-CEL UV_{254}; Macherey-Nagel) with 0.65 M LiCl and visualized by autoradiography.

***In vitro* capped RNA cleavage and RNA elongation reactions.** The determination of Flu cap-dependent endonuclease activity and the subsequent RNA elongation reaction were carried out in a reaction mixture (25 μl) containing 50 mM Tris-HCl (pH 7.9), 0.1 mM ammonium acetate, 5 mM $MgCl_2$, 2.5 mM DTT, 0.1% Nonidet P-40, 8 U of RNasin, 3 to 5 fmol of each ^{32}P-capped RNA (800 cpm/fmol), and an appropriate amount of purified vRNPs without or with ATP, UTP, GTP, or CTP. The reaction mixture was incubated at 30°C for 2 h, and then RNA products were extracted with phenol-chloroform and ethanol precipitated. The RNA products denatured with formamide were electrophoresed in a 20% acrylamide gel containing 8 M urea. After electrophoresis, the gel was dried, and RNAs were visualized by autoradiography. The amount of synthesized RNA was measured with a liquid scintillation counter (LS6000IC; Beckman). The endonuclease activity was represented as a ratio of the amount of cleaved RNAs to that of total capped RNAs, and the RNA elongation efficiency was represented as a ratio of the amount of transcripts to that of total capped RNAs.

Cap-binding assay. UV cross-linking was carried out to measure the cap-binding activity of viral RNA polymerases. A reaction mixture (12 μl) containing